

A New Method to Assess the Jetting Behavior of Drop-on-Demand Ink Jet Fluids

Sungjune Jung[^], Stephen D. Hoath[^], Graham D. Martin[^] and Ian M. Hutchings[^]
Institute for Manufacturing, Department of Engineering, University of Cambridge, 17 Charles Babbage
Road, Cambridge CB3 0FS, United Kingdom
E-mail: imh2@cam.ac.uk

Abstract. We present a new experimental method to assess the jetting performance of fluids for use in drop-on-demand (DoD) ink jet printheads. The oblique collision of two continuous liquid jets leads to the formation of a thin oval liquid sheet bounded by a thicker rim which disintegrates into ligaments and droplets. Under certain conditions the flow structure exhibits a remarkably symmetrical “fishbone” pattern composed of a regular succession of longitudinal ligaments and droplets. For a series of model elastic fluids containing polystyrene (PS) in diethyl phthalate (DEP), and also for solutions of polyethylene oxide (PEO) in glycerol/water, ejected from nozzles with an internal diameter of 0.85 mm, the shape of the fishbone pattern varies strongly with polymer concentration. The same fluids were also used in a Xaar piezoelectric DoD print head to characterize their jetting performance in terms of the maximum ligament length, a crucial parameter in determining the printability of the fluid. There are close similarities between the ligament collapse behaviors in both experiments. Good correlation was found between the maximum included angle of the fishbone pattern and the maximum ligament length in the jetting experiments, which suggests that a test based on oblique impinging jets may be useful in the development of fluids for ink jet printing. © 2011 Society for Imaging Science and Technology.
[DOI: 10.2352/J.ImagingSci.Technol.2011.55.1.010501]

INTRODUCTION

Ink jet printing technology has been widely applied not only to conventional graphics printing but also as an industrial manufacturing process for radio frequency identification (RFID) tags, printed circuit boards (PCBs), and organic electronics such as plastic organic light emitting diodes (P-OLEDs) and organic thin-film transistors (OTFTs), as well as to the deposition of biological material.^{1–6} For optimal performance in drop on demand (DoD) ink jet printing, the fluid should satisfy specific physical properties. In the case of Newtonian fluids which have now been used for more than 30 years, it has been proposed that Z , the inverse of the Ohnesorge number of the fluid [$Z = 1/Oh = (\rho\sigma d)^{1/2}/\eta$ where ρ is the fluid density, σ is its surface tension, η is its viscosity and d is the jet diameter] must lie in the range $1 < Z < 10$ for proper drop formation.⁷ More recently, a printable range of $4 < Z < 14$ has been suggested by considering characteristics such as single droplet

formability, positional accuracy and maximum allowable jetting frequency.⁸

Ink jet printing with non-Newtonian fluids, which is essential for various industrial applications, is significantly affected by the presence of viscoelasticity in the ink as the droplet is formed and ejected in a highly extensional flow. Poor jetting behavior will occur above a certain degree of elasticity, which typically arises from the presence of polymers; such fluids may form jets with very long tails, or the jet may even fail to detach from the nozzle. So far, few studies have been conducted on the printability of viscoelastic fluids. The correlation between filament stretching and jetting performance for viscoelastic fluids has been studied using a modification of a multi-pass rheometer.^{9,10} Apparent extensional viscosities of the fluids were obtained from measurement of the midfilament diameter and the values were found to depend on polymer concentration and Hencky strain. The transient stretching and break-up profiles recorded with this method correlated well with ink jet ligament behavior and the tendency to form satellite drops. Hoath et al. studied jet formation and evolution for dilute polymer solutions. They found that the viscosity measured under low shear-rate conditions showed no correlation with jetting performance, whereas the jetting behavior was well correlated with high frequency rheological properties measured by piezoelectric axial vibration (PAV).¹¹ However, high frequency rheometry involves specialized techniques which are not widely available.

In this article a new method is proposed to assess the jettability of non-Newtonian ink jet fluids, without using an ink jet printhead. An experimental investigation of the formation, destabilization, and atomization of the liquid sheets created by the oblique impact of two laminar jets of a Newtonian liquid has recently been reported.¹² That work focused on the remarkably symmetrical “fishbone” pattern composed of a regular succession of longitudinal ligaments and droplets which is observed in this system under certain flow conditions and which was previously also studied in detail by Bush and Hasha.¹³ The occurrence and shape of the fishbone pattern were found, for Newtonian fluids, to depend strongly on fluid viscosity: in this study, for glycerol/water mixtures, such patterns were only observed for viscosities between 6 and 20 mPa s. In subsequent work¹⁴ it has been shown that, for polymer solutions, development of the

[^]IS&T member

Received Dec. 22, 2009; accepted for publication Aug. 17, 2010; published online Dec. 14, 2010.

1062-3701/2011/55(1)/010501/6/\$20.00.

fishbone pattern was also strongly influenced by the presence of small concentrations of polymer and could be correlated with the elastic component of the complex viscosity as measured by PAV rheometry.

There is an extensive literature on the formation and behavior of the liquid sheets resulting from the collision of jets, and on related aspects of the fluid mechanics of free-surface flows, which have mainly been studied for Newtonian fluids.^{12,13,15,16} The behavior of viscoelastic fluids under these conditions has received rather less attention.^{14,17,18} A fuller discussion of previous relevant work is available from these references; it is the purpose of the present paper to focus on the possibility that the observation of periodic atomization patterns produced by the oblique collision of two viscoelastic liquid jets, i.e., the fishbone patterns, might be used to access rheological information which is relevant to the behavior of the same polymer-containing fluid when it is jetted from a piezoelectric drop-on-demand printhead.

EXPERIMENTAL METHODS

Experimental Fluids

Solutions of polystyrene (PS) in diethyl phthalate (DEP) were formulated to investigate the effects of polymer concentration and molecular weight. DEP (99.5% purity) which is a relatively good solvent for PS at room temperature was purchased from Sigma-Aldrich (Milwaukee, WI), and monodisperse PS was obtained from BASF (Germany). PS with three different molecular weights of 1.10×10^5 , 2.10×10^5 , and 4.88×10^5 g mol⁻¹ was dissolved in DEP with concentrations from 0.01 to 1 wt %. For brevity, these polymers are designated PS 110K, PS 210K and PS 488K, respectively. For these molecular weights the relaxed (fully coiled) end-to-end molecular lengths range from 8 to 17 nm, although since DEP is a good solvent for PS, the unextended molecular lengths would be expected to be somewhat greater. The fully extended chain lengths would be from 0.3 to 1.2 μm. The viscosities were measured with a Viscolite 700 vibrational viscometer (Hydramotion Ltd., U.K.), and lay in the range 11–14 mPa s. Equilibrium surface tension was measured with a bubble pressure tensiometer (SITA pro line t15) and was almost the same (~ 37 mN m⁻¹) for all the PS solutions.

In order to investigate whether solutions of a different polymer also behaved in a similar way, a series of solutions of polyethylene oxide (PEO: Sigma-Aldrich, average molecular weight 1×10^5 g mol⁻¹, designated PEO 100K) was prepared in a glycerol/water solvent (ratio 60%:40% by weight). The PEO concentrations ranged from 0.001 to 1 wt %, and these solutions had zero-shear viscosities between 10 and 13 mPa s and surface tensions of ~ 53 mN m⁻¹.

Experimental Apparatus

Figure 1 shows a schematic diagram of the region where the two jets collide. Fluid from a reservoir was pumped through flexible tubing via a flow meter into a splitter, and divided between two identical stainless steel hypodermic needles (with square ends) with an internal diameter of 0.85 mm.

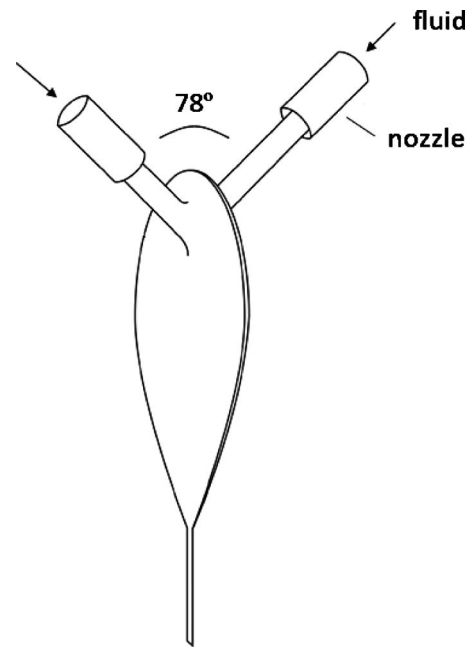


Figure 1. Schematic showing the collision of two liquid jets.

The angle between the axes of the two needles was held constant at 78°, for which the fishbone pattern was found to be best developed for pure DEP and for the pure glycerol/water mixture. The jet lengths, defined as the distances from the ends of the nozzles to the impact point, were 3.5 and 6.5 mm. This asymmetry in nozzle position was required to generate the flow instability needed for a symmetrical fishbone structure, which also required precise alignment of the needles. The rotor-based flow meter with an electronic pulse output was calibrated for each solution by measuring the frequency of the pulses and the fluid volume ejected from the needles over a set time. The jet velocity from the nozzles was varied by changing the speed of the pump, in order to observe the progression of the resulting fluid pattern as it was changed from ~ 1.5 to 6 m s⁻¹. The corresponding ranges of Reynolds number ($Re = \rho dV / \eta$ where V is the jet velocity) and Weber number ($We = \rho d^2 V / \sigma$) were $70 < Re < 700$ and $30 < We < 600$.

Single-flash photography with back illumination was used to capture individual images of the jet interaction region and to extract quantitative information such as the sizes of the resulting droplets and the spacing or angle between the droplet streams. The light source was a xenon lamp with ~ 1 μs flash duration, and the image was captured with a 10 megapixel digital single lens reflex camera (Nikon D40X). The short duration of the flash ensured that there was no significant motion blurring. The axis of the optical system was normal to the fluid sheet. Further details of the experimental method have been published elsewhere.¹²

In order to study the correlation between fishbone patterns formed in the impinging jet experiment and the jetting behavior from a DoD printhead, the fluids were also jetted at room temperature (25°C) from a Xaar XJ126–200 drop-on-demand printhead with a 50 μm nozzle diameter, which produced droplets ~ 80 pL in volume (i.e., ~ 54 μm in di-

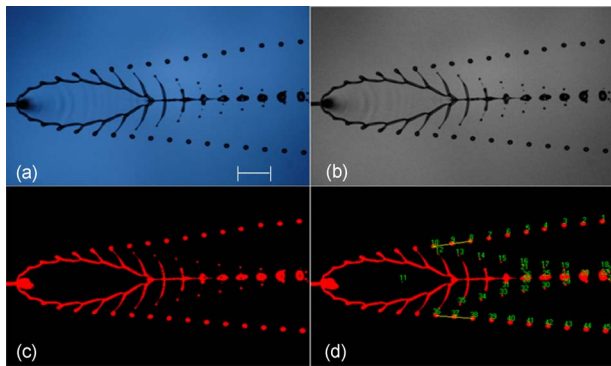


Figure 2. Image processing sequence. (Images are rotated through 90°) (a) 24-bit RGB image; (b) 8-bit gray-scale image; (c) 2-bit binary image; (d) particle analysis. Scale bar: 5 mm

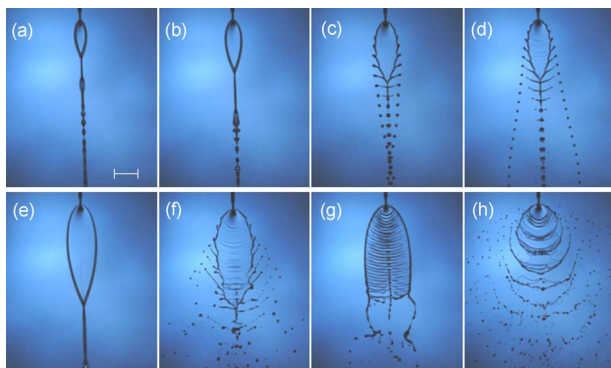


Figure 3. Single-flash images showing the evolution of the fluid sheets formed by impinging jets of a liquid with low elasticity (0.01 wt % PS 488K in DEP). (a, b) fluid chain; (c, d) periodic atomization; (e) smooth single sheet; (f) sheet with fluttering; (g) disintegrating ruffled sheet; (h) violent flapping. Scale bar: 5 mm

ameter). The same pull-push drive waveforms were used throughout, but with the drive level adjusted for each fluid to achieve a constant jet velocity of $\sim 6 \text{ m s}^{-1}$ at 1 mm standoff distance. The jets and drops were analyzed by high-speed imaging, based on very rapid (20 ns) single-flash photography as described previously.¹⁹

Image Processing

Image processing was performed in several steps as shown in Figure 2. An 8 bit grayscale image (b) was obtained by extracting the intensity plane from an original HSI (Hue, Saturation and Intensity) image (a). In the next step, thresholding was applied to isolate objects of interest in the image. Through this process, the grayscale image with pixel values ranging from 0 to 255 was converted into a binary image with pixel values of 0 or 1 (c). Binary morphological operations were also performed in order to remove unwanted information. Finally, particle analysis was carried out to make measurements such as drop diameter, drop spacing and stream angle, defined by four points (d).

RESULTS AND DISCUSSION

Observations

As seen in Figure 3, the collision of two jets of a dilute

solution of PS 488K (0.01 wt % in DEP) with low elasticity results in the formation of various fluid patterns with increasing flow velocity: oscillating streams (not shown); fluid chain [Figs. 3(a) and 3(b)]; periodic atomization (the ‘fishbone’ form) (c and d); smooth single sheet (e); sheet with fluttering (f); disintegrating ruffled sheet (g); and violent flapping (h). Initially, the successive sheets in the fluid chain in Figs. 3(a) and 3(b) consist of thin oval fluid regions each bounded by a thicker rim. The oval film becomes larger as the flow rate increases. Small perturbations on the rim start to appear and gradually grow, leading to periodic detachment of droplets. As the flow rate is increased, the pattern adopts the characteristic fishbone form, consisting of a fluid sheet, a series of ligaments and droplets [Figs. 3(c) and 3(d)]. The ligaments elongate, and the degree of that extension depends on both the viscosity and elasticity of the fluid. Under these conditions, the droplets generated are $\sim 1 \text{ mm}$ in diameter and traveling at $\sim 2 \text{ m s}^{-1}$. The speed of extension of the ligaments is $\sim 0.8 \text{ m s}^{-1}$. When this pattern reaches its maximum extent [Fig. 3(d)], it suddenly converts into a stable single sheet larger than that seen in the fluid chain, and then on further increase in velocity becomes unstable again, giving rise to random droplets. As the jet velocity is increased further, the sheet becomes ruffled, forming a disintegrating ruffled sheet with a stable rim. Finally, violent flapping ensues at very high flow rates.

Effects of Viscoelasticity on the Fishbone Pattern

The effects of fluid viscoelasticity on the flow structures are most clearly observed in the fishbone regime. As discussed above and shown in Figs. 3(c) and 3(d), in this regime the flow pattern consists of a single oval fluid sheet bounded by a thicker rim which becomes unstable, forming ligaments and droplets. The velocity profile within the two original jets at their point of impact plays a key role in the initiation of the instability on the rim of the fluid sheet. The instability starts from the upper part of the sheet and continues to develop around the rim on each side, forming longitudinal ligaments which eventually break up into droplets. The extension and break-up of the ligaments is controlled by similar processes to those which influence the behavior of jets from a drop-on-demand printhead, although the size and timescales both differ. How the changes in various parameters such as jet length, alignment or fluid properties influence the form of the fishbone pattern, and the origin and mechanism of the periodic atomization of the sheet, are discussed elsewhere.¹²

The concept of the ‘fishbone angle’ is useful to describe the degree of development of the fishbone structure which varies with the elasticity of the fluid.¹⁴ The fishbone angle is defined as the angle (θ) between the trajectories of the droplets on each side of the central spine as illustrated in Figure 4. The maximum fishbone angle is the angle (θ_{max}) at which the flow structure is fully extended, just before it changes to the next regime [i.e., the smooth fluid sheet shown in Fig. 3(e)]. For precise and reliable measurement through the imaging processing technique, the two consecutive droplets were selected which had just detached from the ligaments on

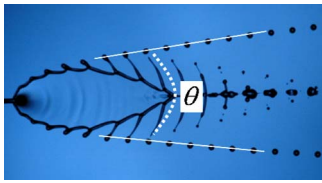


Figure 4. Definition of fishbone angle as the angle (θ) between the trajectories of the droplets on each side of the spine. Maximum fishbone angle (θ_{\max}) is the value of θ when the flow structure is fully extended, just before it changes to the next regime [i.e., the smooth fluid sheet shown in Fig. 3(e)].

each side of the pattern. The computed centers of mass of these four droplets were used to define the fishbone angle.

Correlation of θ_{\max} with Jetting Performance

Previous work has demonstrated that the elasticity of the fluid, as measured by high-speed rheometry, is correlated with the value of θ_{\max} .¹⁴ Increasing elasticity results in a decrease in θ_{\max} . In order to examine the correlation between θ_{\max} and the performance of each fluid in a drop-on-demand printhead, the maximum ligament length (MLL) was measured from an image captured at the point at which the jets had just detached from the nozzle plane. MLL is one of the most important parameters which determines the printability of a fluid. Many printers operate with about 1 mm stand-off distance, so that 1 mm is the maximum practical ligament length for successful printing, although a maximum length of 0.4 to 0.6 mm might be preferable for better print quality.

Figures 5(a) and 5(b) shows typical images of jets formed from a dilute solution (0.01 wt % PS 110K in DEP) and from a solution close to the limit of printability (0.4 wt % PS 110K). Once jets become detached from the nozzle plate they will eventually either collapse to form a single drop or break up into multiple satellites; in extreme cases they may never detach from the nozzle plate, as shown for a higher polymer concentration (1 wt % PS 110K) in Fig. 5(c). Long ligaments that do not become detached may subsequently retract fully into the nozzle, while for even higher polymer concentrations the fluid may never emerge from the nozzle. For cases where ligaments and drops detached from the nozzle, the size of the main drop was found to be slightly increased (by a few percent at most) by an increase in polymer concentration. The total amount of fluid ejected from the nozzle, however, including the volume in the ligament, was significantly increased as the drive voltage had to be increased to achieve the target speed of 6 m s^{-1} at a standoff distance of 1 mm.

Figure 6 compares the values of θ_{\max} as defined above with the values for the PS and PEO solutions as a function of polymer concentration. The two sets of measurements show remarkably consistent trends for all the molecular weights and for both the polymer/solvent systems studied. While the values of θ_{\max} for concentrations below a certain level (which varied somewhat for the different polymers) were approximately constant, above those concentrations, for all the polymers, θ_{\max} decreased with increasing polymer

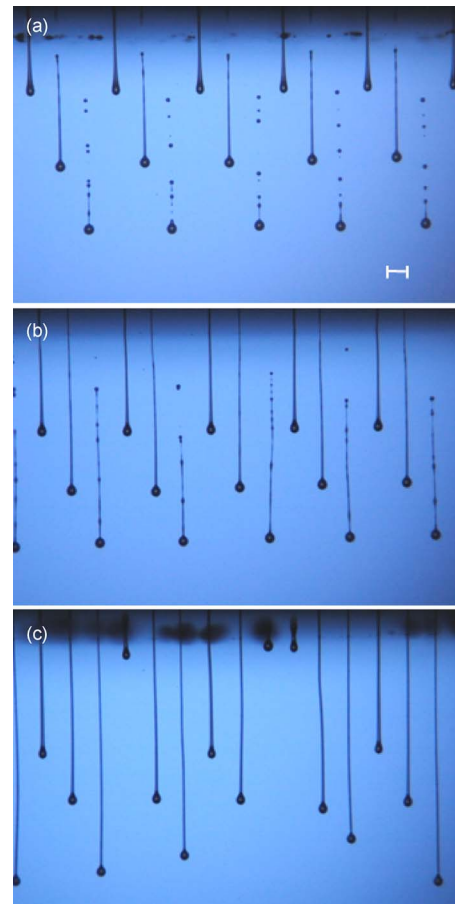


Figure 5. Examples of jets emitted from a drop-on-demand printhead: (a) dilute polymer solution (0.01 wt % PS 110K); (b) more concentrated solution which still forms detached jets (0.4 wt % PS 110K); (c) even more concentrated solution for which the jets do not detach (1 wt % PS 110K). Scale bar: $100 \mu\text{m}$

concentration. The higher molecular weight PS solutions exhibited a more rapid change in fishbone angle. The ink jet ligament length changed in a similar way; it was essentially constant for polymer concentrations below the same critical level and increased rapidly with increasing concentration. The higher molecular weight PS solutions showed a greater dependence of ligament length on concentration. These changes probably occur as the solutions move from a “dilute” regime into a “semidilute” regime, where polymer chain-to-chain interactions start to occur. We may conclude that intermolecular interactions in these polymer solutions strongly influence the ligament length under printing conditions in the same way that they affect the fishbone structure, despite the differences in timescale and drop/ligament size.

These results suggest that the observation of the interaction of colliding continuous jets may be useful to obtain information which is relevant to the dynamics of drop formation and jet breakup in ink jet printing. From measurements of θ_{\max} for ink formulations containing different concentrations of polymer, it should be possible to identify the level at which viscoelastic effects will significantly affect jet-

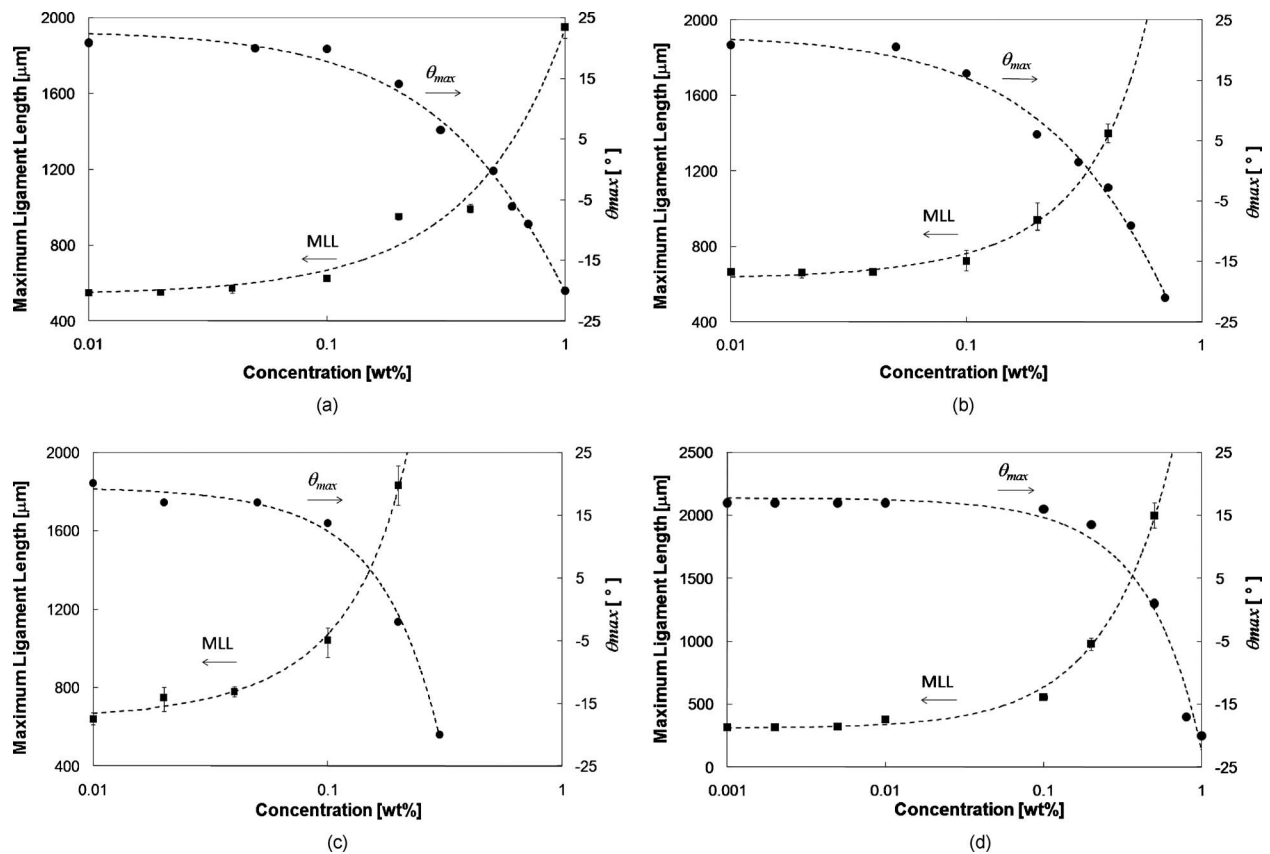


Figure 6. Comparison between the variation in maximum ligament length (MLL) and maximum fishbone angle (θ_{max}) with polymer concentration for solutions of PS with different molecular weights and for solutions of PEO 100K. (a) PS 110K; (b) PS 210K; (c) PS 488K; (d) PEO 100K.

tability. The method might thus be used, after suitable calibration experiments, as a guide to the maximum polymer content in fluids intended for ink jet printing.

CONCLUSIONS

We suggest that information about the printability of a viscoelastic (e.g., polymer-containing) fluid can be obtained by observation of the symmetrical “fishbone” structure which is generated under certain conditions by the oblique collision of two impinging jets of the fluid. We have shown that viscoelasticity has a strong effect on the break-up of a fluid sheet. As the elasticity of the fluid grows, the maximum angular extent of the fluid fishbone structure was found to decrease. Fluid fishbone patterns can be used to distinguish viscoelastic regimes in terms of degree of polymer dilution. Good correlation is found between the maximum fishbone angle (i.e., the maximum included angle between the droplet streams in the fishbone pattern) and the maximum ligament length measured in jetting experiments from a DoD printhead, which suggests that the fishbone phenomenon may provide a simple and useful tool to explore the upper limit of polymer concentration in ink jet printing fluids.

ACKNOWLEDGMENTS

This research was partly supported by the UK EPSRC and industrial partners in the Next Generation Ink Jet Printing

Consortium. S.J. thanks Cambridge Display Technology Ltd. for financial support.

REFERENCES

- G. D. Martin, S. D. Hoath, and I. M. Hutchings, “Ink jet printing - the physics of manipulating liquid jets and drops”, *J. Phys.: Conf. Ser.* **105**, 012001 (2008).
- V. Subramanian, J. Chang, B. Mattis, S. Molesa, D. Redinger, A. D. L. F. Vornbrock, and S. K. Volkman, “All-printed electronics: materials, devices, and circuit implications”, *Proc. IS&T's 2nd International Conference on Digital Fabrication Technologies* (IS&T, Springfield, VA, 2006) p.21.
- W.-K. Hsiao, G. D. Martin, S. D. Hoath, and I. M. Hutchings, “Ink jet printing for direct mask deposition in printed circuit board fabrication”, *J. Imaging Sci. Technol.* **53**, 050304 (2009).
- B.-J. de Gans, P. C. Duineveld, and U. S. Schubert, “Ink jet printing of polymers: State of the art and future developments”, *Adv. Mater. (Weinheim, Ger.)* **16**, 203 (2004).
- Y. Noh, N. Zhao, and H. Sirringhaus, “Downscaling of self-aligned, all-printed polymer thin-film transistors”, *Nat. Nanotechnol.* **2**, 784 (2007).
- P. Calvert, “Printing cells”, *Science* **318**, 208 (2007).
- N. Reis, C. Ainsley, and B. Derby, “Ink jet delivery of particle suspensions by piezoelectric droplet ejectors”, *J. Appl. Phys.* **97**, 094903 (2005).
- D. Jang, D. Kim, and J. Moon, “Influence of fluid physical properties on ink jet printability”, *Langmuir* **25**, 2629 (2009).
- T. R. Tuladhar and M. R. Mackley, “Filament stretching rheometry and break-up behaviour of low viscosity polymer solutions and ink jet fluids”, *J. Non-Newtonian Fluid Mech.* **148**, 97 (2008).
- D. C. Vadillo, T. R. Tuladhar, A. C. Mulji, M. R. Mackley, S. Jung, and S. D. Hoath, “Evaluation of the ink jet fluid’s performance using the ‘Cambridge Trimaster’ filament stretch and break-up device”, *J. Rheol.* **54**, 261 (2010).

- ¹¹ S. D. Hoath, I. M. Hutchings, G. D. Martin, T. R. Tuladhar, M. R. Mackley, and D. C. Vadillo, "Links between fluid rheology and drop-on-demand jetting and printability", *J. Imaging Sci. Technol.* **53**, 041208 (2009).
- ¹² S. Jung, S. D. Hoath, G. D. Martin, and I. M. Hutchings, "Atomization patterns produced by the oblique collision of two Newtonian liquid jets", *Phys. Fluids* **22**, 042101 (2010).
- ¹³ J. W. M. Bush and A. E. Hasha, "On the collision of laminar jets: fluid chains and fishbones", *J. Fluid Mech.* **511**, 285 (2004).
- ¹⁴ S. Jung, S. D. Hoath, G. D. Martin, and I. M. Hutchings, "Experimental study of atomization patterns produced by the oblique collision of two viscoelastic liquid jets", *J. Non-Newtonian Fluid Mech.* (2011) (in press).
- ¹⁵ C. Clanet, "Waterbells and liquid sheets", *Annu. Rev. Fluid Mech.* **39**, 469 (2007).
- ¹⁶ R. Li and N. Ashgriz, "Characteristics of liquid sheets formed by two impinging jets", *Phys. Fluids* **18**, 087104 (2006).
- ¹⁷ A. N. Rozhkov, "Dynamics and breakup of viscoelastic liquids (A review)", *Fluid Dyn.* **40**, 835 (2005).
- ¹⁸ E. Miller, B. Gibson, E. McWilliams, and J. P. Rothstein, "Collision of viscoelastic jets and the formation of fluid webs", *Appl. Phys. Lett.* **87**, 014101 (2005).
- ¹⁹ I. M. Hutchings, G. D. Martin, and S. D. Hoath, "High speed imaging and analysis of jet and drop formation", *J. Imaging Sci. Technol.* **51**, 438 (2007).